Int. J. Heat Mass Transfer. Vol. 17, pp. 1019–1028. Pergamon Press 1974. Printed in Great Britain

CONDENSATION FROM A TURBULENT STREAM ONTO A VERTICAL SURFACE

W. P. JONES and U. RENZ
Lehrstuhl für Technische Thermodynamik, Rheinisch-Westfälische Technische Hochschule, 5100 Aachen, Germany

(*Received* 27 *August* 1973)

Abstract—The paper presents some numerical predictions of the turbulent flow of a mixture of CCl_4 vapour and air over a vertical plate onto which the vapour condenses. For the vapour–air mixture, the set of partial differential equations governing the conservation of momentum, species and enthalpy were solved by a finite-difference procedure. The liquid/air–vapour interface boundary conditions were obtained from a modified Nusselt approximation for the liquid film.

Results were obtained with three versions of the Prandtl mixing length model of turbulence and a model in which the turbulent viscosity is determined from solution of transport equations for the turbulent kinetic energy and dissipation rate of turbulence energy—the $k-\varepsilon$ model. Of the mixing length models that of Cebeci led to the closest agreement with measurements. The $k-\varepsilon$ model predictions are also in close accord with experiment.

NOMENCLATURE

A^+, a constant appearing in the Van Driest formula for effective viscosity;
c_p, specific heat at constant pressure;
c_{ε_1}, c_{ε_2}, c_μ, empirical constants appearing in $k-\varepsilon$ turbulence model;
g, gravitational acceleration;
h, specific enthalpy;
k, turbulence kinetic energy;
l, mixing length;
m, mass concentration of CCl_4;
$\dot{m}_I''$, condensation rate, $\rho_I v_I$;
m_+, dimensionless condensation rate, $\dot{m}_I''/\sqrt{(\tau_I\rho)}$;
M, mean condensation rate over measuring section,

$$\frac{\frac{1}{L}\int_0^L \dot{m}_I''\,\mathrm{d}x}{\rho_G u_G};$$

$\dot{q}''$, heat-transfer rate;
R_T, Reynolds number of turbulence;
St_h, mean Stanton number for heat transfer,

$$\frac{\frac{1}{L}\int_0^L \dot{q}_v''\,\mathrm{d}x}{\rho_G u_G c_{p_G}(T_I - T_G)};$$

St_m, mean Stanton number for mass transfer,

$$\frac{M(1-m_I)}{(m_G - m_I)};$$

T, temperature;
u, v, flow velocities in the x and y directions;
x, y, coordinate axes measured parallel and normal to the plate respectively;
y^+, dimensionless value of y, $\dfrac{y\sqrt{(\tau_I\rho)}}{\mu}$.

Greek symbols

δ, thickness of vapour–air boundary layer;
δ_1, displacement thickness of vapour–air boundary layer,

$$\int_{\delta_L}^{\infty}\left(1-\frac{\rho u}{\rho_G u_G}\right)\mathrm{d}y;$$

δ_L, liquid film thickness;
ε, rate of dissipation of turbulence kinetic energy;
κ, Von Kármán mixing length constant;
λ, thermal conductivity;
μ, dynamic viscosity;
ρ, density;
σ, Prandtl–Schmidt number;
τ, total shear stress, $\mu(\partial u/\partial y) - \rho\overline{u'v'}$;
τ_+, dimensionless shear stress, τ/τ_I;
ϕ, heat of vaporization.

Subscripts

eff, effective;
G, free stream;
i, inner region of vapour–air boundary layer;

I, vapour–air/liquid interface;
L, liquid;
o, outer region of vapour–air boundary layer;
T, turbulent;
v, vapour–air;
w, wall.

INTRODUCTION

THE PROBLEM of condensation of a vapour onto a vertical surface is one which has been the subject of many theoretical studies since the pioneering analysis of Nusselt [1]. For the gravity-flow laminar film where a laminar vapour–gas boundary layer arises from natural convection the governing partial differential equations admit a similarity solution and the resulting ordinary differential equations may be integrated either analytically or numerically, see for example [2]. In the case of turbulent flow a similarity analysis is not possible and there is the additional problem of providing a model for the turbulence transport processes. Perhaps for these reasons most previous analyses have been concerned with the more tractable laminar flow case and comparatively little attention has been paid to the more practically significant turbulent flow.

Most industrial situations where the boundary-layer approximation is appropriate involve a forced vapour–gas convection flow which will usually also be turbulent. However, whether the flow is laminar or turbulent a proper analytic treatment requires solution of a coupled set of partial differential equations which cannot be reduced to ordinary differential equations. The development, in recent years, of a number of finite-difference schemes for solving the partial differential boundary-layer equations provides a means whereby such a treatment is now possible. Recently Denny *et al.* [3] have followed this approach to study the forced laminar flow of a stream–air mixture over a vertical plate. However, it seems that such an approach has not yet been applied to the turbulent case and it is to this which we now direct attention.

The present contribution

Recently Dallmeyer [4] has presented the results of an experimental investigation of a forced turbulent flow of a mixture of air and CCl_4 vapour over a vertical flat plate onto which the vapour condenses. The experimental set up was such that the vapour–air boundary layer was always fully turbulent but the liquid film developing along the plate remained laminar everywhere.

The study covered a wide range of heat transfer and condensation rates and profiles of mean velocity, temperature and concentration were measured for selected experimental runs.

It is the purpose of the present paper to describe the results of an investigation into the applicability of a number of previously proposed turbulence models to the above flow system. Predictions have been made using the modified van Driest mixing length models of Cebeci [5], Kays [6], Launder and Priddin [7] and the model of reference [8]. In the latter model the turbulent viscosity is obtained from the solution of transport equations for the turbulence kinetic energy and dissipation rate of turbulence energy. A comparison is drawn between the experimental results and the predictions so obtained. The effect of neglecting the liquid film and the buoyancy forces from the air–vapour boundary layer analysis is also explored.

Theoretical considerations

A schematic outline of the flow system is shown in Fig. 1. A mixture of air and CCl_4 vapour flows vertically over a vertical plate. The liquid film of condensate flows down the plate under the influence of gravity and surface friction forces. Corresponding to the experimental situation the liquid film is laminar everywhere and surface waves are assumed absent. The CCl_4 vapour–air boundary layer developing over the liquid film is turbulent from the leading edge of the plate.

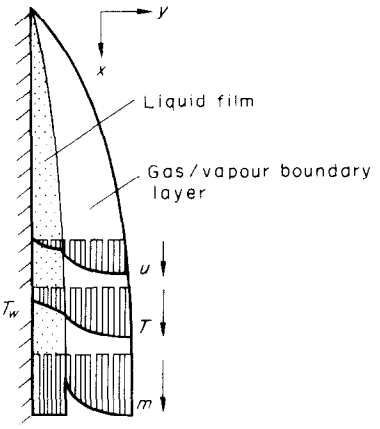

FIG. 1. Outline of the physical situation.

The liquid film. The liquid film properties are evaluated at the arithmetic mean temperature of the film and, following Nusselt, the convection terms are neglected from the enthalpy and momentum equations. With this assumption the equations reduce to:

$$\mu \frac{d^2u}{dy^2} + g(\rho - \rho_\infty) = 0 \tag{1}$$

$$\frac{d^2T}{dy^2} = 0. \tag{2}$$

To the above equations the mass conservation equation must be added:

$$\frac{\partial u}{\partial x}+\frac{\partial v}{\partial y}=0. \tag{3}$$

The CCl_4 vapour–air boundary layer

For the vapour–air boundary layer the equations for the conservation of mass, momentum, enthalpy and species may be written:

$$\frac{\partial \rho u}{\partial x}+\frac{\partial \rho v}{\partial y}=0 \tag{4}$$

$$\rho u\frac{\partial u}{\partial x}+\rho v\frac{\partial u}{\partial y}=\frac{\partial}{\partial y}\left\{\mu_{\text{eff}}\frac{\partial u}{\partial y}\right\}+g(\rho-\rho_\infty) \tag{5}$$

$$\rho u\frac{\partial h}{\partial x}+\rho v\frac{\partial h}{\partial y}=\frac{\partial}{\partial y}\left\{\frac{\mu_{\text{eff}}}{\sigma_{\text{eff},h}}\frac{\partial h}{\partial y}\right\}+\frac{\partial}{\partial y}\left\{\frac{\mu_{\text{eff}}}{\sigma_{\text{eff},m}}\left(1-\frac{\sigma_{\text{eff},m}}{\sigma_{\text{eff},h}}\right)(h_{CCl_4}-h_{\text{air}})\frac{\partial m}{\partial y}\right\} \tag{6}$$

$$\rho u\frac{\partial m}{\partial x}+\rho v\frac{\partial m}{\partial y}=\frac{\partial}{\partial y}\left\{\frac{\mu_{\text{eff}}}{\sigma_{\text{eff},m}}\frac{\partial m}{\partial y}\right\} \tag{7}$$

where

$$\mu_{\text{eff}}=\mu+\mu_T \quad \text{and} \quad \sigma_{\text{eff}}=\frac{\mu_{\text{eff}}}{\frac{\mu}{\sigma}+\frac{\mu_T}{\sigma_T}}.$$

To complete the description of the vapour–air boundary layer the turbulent transport properties must be specified by means of a turbulence model. In the present contributions we explore the implications of the turbulence models outlined below.

THE MIXING LENGTH MODELS

The mixing length hypothesis of Prandtl can be expressed as

$$\mu_T=\rho l^2\left|\frac{\partial u}{\partial y}\right| \tag{8}$$

where l is the mixing length which must be specified in terms of the flow geometry. For the near wall region of a boundary layer developing along a smooth surface van Driest [9] proposed that the mixing length varied according to the formula:

$$l=\kappa y(1-\exp\{-y^+/A^+\}). \tag{9}$$

With the constants κ and A^+ assigned the values 0·4 and 26, the expression was found to lead to predictions in excellent accord with experiment for constant fluid property flows with small pressure gradient and small surface mass-transfer rates. The model has also been found to give accurate predictions for flows in which fluid property variations are pronounced, e.g. [10] and [11]. However in situations where appreciable pressure gradients and/or surface mass-transfer rates occur modification of the van Driest mixing length expression is necessary. In the past there have been many suggested variations of the van Driest formula: nearly all these proposals can be interpreted as accounting for the effects of pressure gradient and mass transfer by allowing A^+ to vary. For example in references [12] and [13] A^+ was calculated as a function of dimensionless pressure gradient and the model used to successfully predict heat-transfer rates to strongly accelerated, (i.e. large negative pressure gradient) boundary layers. However we are here concerned with flows with mass transfer and the authors have selected as appropriate the proposals of Cebeci [5], Kays [6] and Launder and Priddin [7]. The models have been constructed with reference to measurements made in boundary layers with surface suction and negligible variation in fluid properties. It is our purpose here to check and compare their applicability to condensation problems where large fluid property variations may arise. The main features of the models are shown in Table 1.

The $k-\varepsilon$ turbulence model

Recently one of the authors has proposed [8] a turbulence model wherein turbulence is assumed to be completely specified by a characteristic time and length

Table 1. Main features of the mixing-length models

Author	Inner region	Outer region	Matching point
Cebeci [5]	$l_i=\kappa y[1-\exp(-y_+/A_+)]$ where $\kappa=0{\cdot}40$, $A_+=26/\exp(5{\cdot}9\,m_+)$	$\mu_T=\dfrac{0{\cdot}0168\,\rho_G u_G \delta_1}{[1+5{\cdot}5(y/\delta)^6]}$	$\mu_{T_i}=\mu_{T_0}$
Kays [6]	$l_i=\kappa y[1-\exp(-y_+/A_+)]$ where $\kappa=0{\cdot}44$, $A_+=27/[\tau_+^{1/2}(1+5{\cdot}15\,m_+)]$	$l_0=l_{\max}=0{\cdot}09\,\delta$	$l_i=l_{\max}$
Launder and Priddin [7]	$l_i=\kappa y[1-\exp(-y_+/A_+)]$ where $\kappa=0{\cdot}41$, $A_+=26/\tau_+^{3/2}$	$l_0=l_{\max}=0{\cdot}075\,\delta$	$l_i=l_{\max}$

scale. These time and length scales are obtained from solution of transport equations for the turbulent kinetic energy and the dissipation rate of turbulence energy. The model contains proposals for the way in which molecular viscosity exerts direct influence on the turbulence when the turbulence Reynolds number is low and hence may be applied to both the viscous sublayer and fully turbulent regions of the boundary layer. The model has been applied to the successful prediction of hydrodynamic and heat-transfer aspects of strongly accelerated boundary layers (i.e. laminarization) [14] and also to flows with surface mass transfer and to flow in ducts at low Reynolds numbers [15]. A full description together with some explanation of the model is given in references [14] and [15] and here we limit ourselves to re-stating the model-equations

Turbulence kinetic energy

$$\rho u\frac{\partial k}{\partial x}+\rho v\frac{\partial k}{\partial y}=\frac{\partial}{\partial y}\left\{\left(\mu+\frac{\mu_T}{\sigma_k}\right)\frac{\partial k}{\partial y}\right\}+\mu_T\left(\frac{\partial u}{\partial y}\right)^2-\rho\varepsilon-2{\cdot}0\mu\left(\frac{\partial\sqrt{k}}{\partial y}\right)^2. \quad (10)$$

Turbulence dissipation rate

$$\rho u\frac{\partial\varepsilon}{\partial x}+\rho v\frac{\partial\varepsilon}{\partial y}=\frac{\partial}{\partial y}\left\{\left(\mu+\frac{\mu_T}{\sigma_\varepsilon}\right)\frac{\partial\varepsilon}{\partial y}\right\}+2{\cdot}0\frac{\mu}{\rho}\mu_T\left(\frac{\partial^2u}{\partial y^2}\right)^2+c_{\varepsilon_1}\frac{\varepsilon}{k}\mu_T\left(\frac{\partial u}{\partial y}\right)^2-c_{\varepsilon_2}\rho\frac{\varepsilon^2}{k} \quad (11)$$

where

$$\mu_T=c_\mu\rho\frac{k^2}{\varepsilon}$$

$$c_\mu=0{\cdot}09\exp[-2{\cdot}5/(1+R_T/50)]$$

$$c_{\varepsilon_1}=1{\cdot}55;\quad c_{\varepsilon_2}=2{\cdot}0[1-0{\cdot}3\exp(-R_T^2)]$$

$$\sigma_k=1{\cdot}00;\quad \sigma_\varepsilon=1{\cdot}3$$

and

$$R_T=\rho\frac{k^2}{\mu\varepsilon}.$$

Equations (1)–(7) are subjected to the following boundary conditions:

at $y=0$, $u=0$ and $T=T_w$

at $y=y_G$, $u=u_G$, $T=T_G$ and $m=m_G$.

For the predictions made with the $k-\varepsilon$ turbulence model the following conditions were imposed on equations (10) and (11)

at $y=\delta_L$, $k=\varepsilon=0$

at $y=y_G$

$$\begin{cases} u_G\dfrac{\mathrm{d}k_G}{\mathrm{d}x}=-\varepsilon_G \\ u_G\dfrac{\mathrm{d}\varepsilon_G}{\mathrm{d}x}=-c_{\varepsilon_2}\dfrac{\varepsilon_G^2}{k_G}. \end{cases}$$

The turbulent Prandtl and Schmidt numbers

The mixing length model of Kays [6] contains a proposal for the variation of the turbulent Prandtl–Schmidt number across the boundary layer as a complex function of mass-transfer rate and normal distance. However in all the other calculations the turbulent Prandtl and Schmidt numbers were assigned the constant value of 0·9.

Thermophysical properties

Vapour–gas mixture. The density was calculated from the Ideal Gas Law. The specific heat, viscosity, thermal conductivity of both components and the vapour pressure and heat of vaporisation of CCl_4 were evaluated from best fit polynomials to the tabulated values quoted in *VDI-Wärmeatlas* [16]. The transport properties of the mixture were calculated from approximate formulae derived from the kinetic theory of gases and given by Reid and Sherwood [17]. The diffusion coefficient of CCl_4 in air was obtained from data reported by Smits [18].

Liquid CCl_4. The density and viscosity were obtained from the tabulated data reported in *VDI-Wärmeatlas* and the thermal conductivity from the data of Touloukian [19].

Method of solution

The conditions at the vapour–air/liquid interface are given by:

$$y=\delta_L,\qquad u_L=u_v=u_I$$

$$T_L=T_v=T_I$$

$$\mu\left.\frac{\partial u}{\partial y}\right|_L=\mu\left.\frac{\partial u}{\partial y}\right|_v=\tau_I$$

$$\dot m_I''=\frac{1}{m_I-1}\frac{\mu}{\sigma_m}\left.\frac{\partial m}{\partial y}\right|_I$$

$$\lambda\left.\frac{\partial T}{\partial y}\right|_L=\lambda\left.\frac{\partial T}{\partial y}\right|_v-\dot m_I''\phi=-\dot q_w''.$$

In addition it is assumed that the interface exhibits negligible departure from thermodynamic equilibrium thus allowing the interface species concentration be be calculated.

Equations (1)–(3) may be integrated to yield:

$$u_I = \frac{\tau_I}{\mu_L}\delta_L + \frac{g}{\mu_L}(\rho_L - \rho_\infty)\frac{\delta_L^2}{2}$$

$$T_I = T_w - \frac{\delta_L}{\lambda}\dot{q}_w''$$

$$\dot{m}_I'' + \frac{\mathrm{d}}{\mathrm{d}x}\int_0^{\delta_L x} \rho_L u \,\mathrm{d}y = 0.$$

The problem is now reduced to that of solving the partial differential transport equations (4)–(7) (plus equations (10) and (11) for the $k-\varepsilon$ model predictions) subject to the complex set of boundary conditions stated above. This coupled set of partial differential equations is solved by a modified version of the finite-difference procedure of Patankar and Spalding [20] in which 100 cross-stream intervals are employed, approximately half of which are concentrated in the 10 per cent of the boundary layer closest to the wall.

Because of the strong coupling between the interface species concentration, temperature and condensation rate it was found necessary to develop an iterative procedure to obtain completely stable solutions for all the runs considered and some re-arrangement of the method is desirable. In the published versions of the Patankar–Spalding finite difference procedure the finite difference coefficients are calculated for all the variables before the downstream values are computed. However, for the present problem it is advantageous to modify the method. The finite difference coefficients are calculated for only one of the dependant variables. The finite different equations are then solved for the downstream values of this variable and these are used, together with the values of the other dependant variables at the upstream station, to calculate the coefficients for the next dependant variable, and so on.

After specification of the initial profiles of the dependant variables the numerical solution is advanced step by step as follows:

1. Assign the interfacial species concentration and the condensation rate their upstream values.
2. Calculate the finite difference coefficients for the species concentration using the upstream values of the other variables.
3. Solve the resulting algebraic equations to give a new species concentration profile.
4. Calculate a new value of the condensation rate from the new concentration profile.
5. Calculate new values of the interface temperature and enthalpy (using the upstream value of $(\mu/\sigma_h)(\partial T/\partial y)|_I$) and hence the interface species concentration.
6. Steps 2 to 5 are then repeated until no significant change in either m_I or $\dot{m}_I''$ occurs.
7. Complete the solution for the remaining dependant variables without any further iteration.

The procedure described above converges very rapidly and (for runs where a non-iterative solution was possible) resulted in only moderate increases in computation time; typically of the order of 10 per cent. The solutions so obtained are very stable and effectively independant of forward step size.

For the initial profiles of u, k and ε required to start the computations, estimated "fully turbulent" profiles were utilized. The calculations were started near the leading edge of the plate; as a result the predicted heat-transfer and mass-transfer rates in the region of interest were found to be little influenced by the initial conditions.

COMPARISON OF PREDICTIONS WITH EXPERIMENTS

We now turn to the comparison between our predictions and the experimental results of Dallmeyer [4]. Dallmeyer's measurements were made over the final 100 mm of a 300 mm long vertical plate over which flowed a condensing mixture of air and CCl_4 vapour. The vapour–air boundary layer developing along the plate was "tripped" by means of a transition device placed near the leading edge of the plate. The liquid film was maintained laminar by sucking off the condensate at intervals of 100 and 200 mm along the plate. Measurements of averaged (over the measuring section) heat-transfer and mass-transfer rates were then obtained by balance.

The predictions of mean velocity, temperature and concentration profiles obtained with the three mixing length models are compared with measured profiles in Figs. 2–7. Figures 2–4 correspond to the flow where M equals 0·0017 and Figs. 5–7 to the higher condensation rate where M equals 0·0032. This latter value of M, it is worth noting, corresponds to a mass-transfer rate some 50 per cent larger than the largest value obtained in experimental studies of flows with surface suction on which the models are based.

It can be seen from the figures that the models of Cebeci and Kays both lead to predicted profiles which are in acceptable agreement with the measurements for both condensation rates. In the case of Cebeci's model the good agreement is also borne out in the predicted values of averaged (over the test section) heat and mass-transfer rates which are in excellent accord with the measurements, e.g. see Table 2. With Kays' model the agreement is not so good and the predicted and measured rates disagree by an amount which increases with increasing condensation rate, e.g. for $M = 0{\cdot}0032$ the Stanton numbers for heat transfer and mass transfer are unpredicted by about 15 per cent.

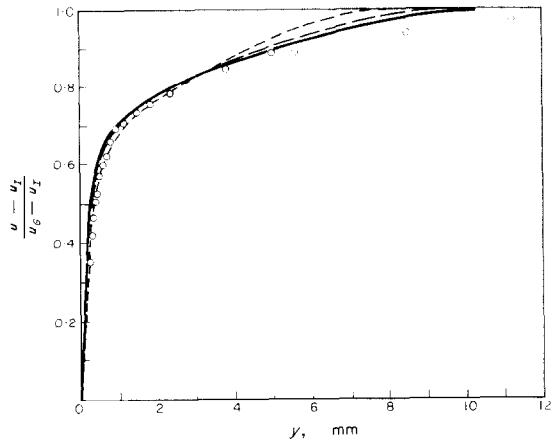

FIG. 2. Velocity profile. Run No. 120. $M = 0{\cdot}0017$. —— Cebeci model, ——— Kays model, -- Launder *et al.* model. ○ Experiment.

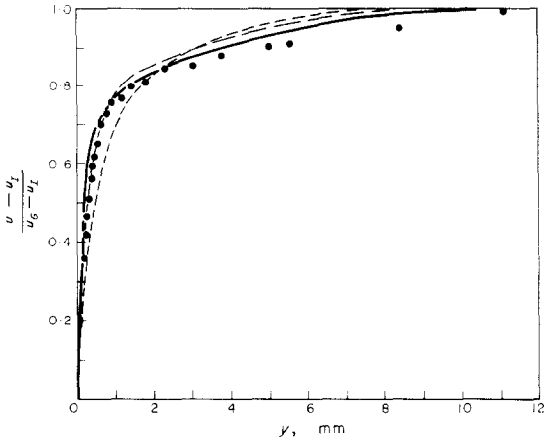

FIG. 5. Velocity profile. Run No. 139, $M = 0{\cdot}0032$. —— Cebeci model; ——— Kays model; -- Launder *et al.* model; ● Experiment.

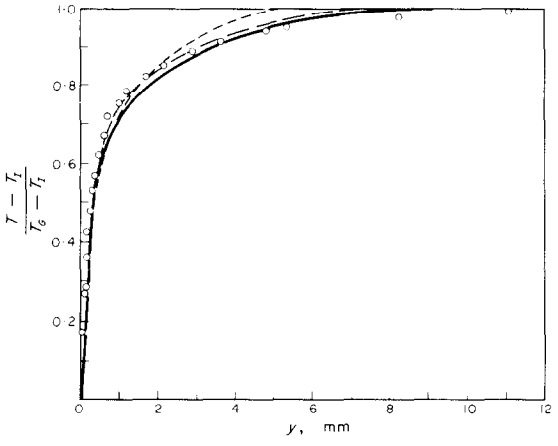

FIG. 3. Temperature profile. Run No. 120, $M = 0{\cdot}0017$. — Cebeci model, - — Kays model, -- Launder *et al.* model. ○ Experiment.

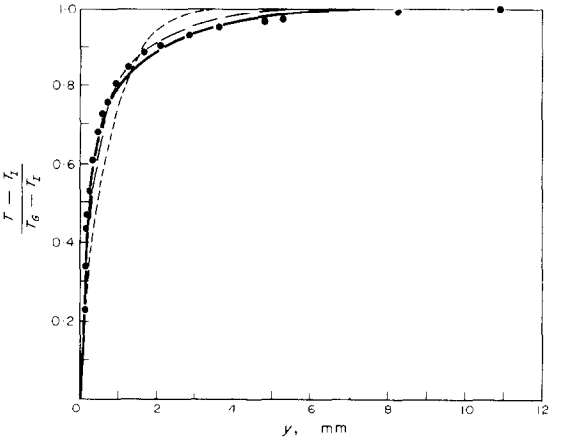

FIG. 6. Temperature profile. Run No. 139, $M = 0{\cdot}0032$. —— Cebeci model; ——— Kays model; -- Launder *et al.* model; ● Experiment.

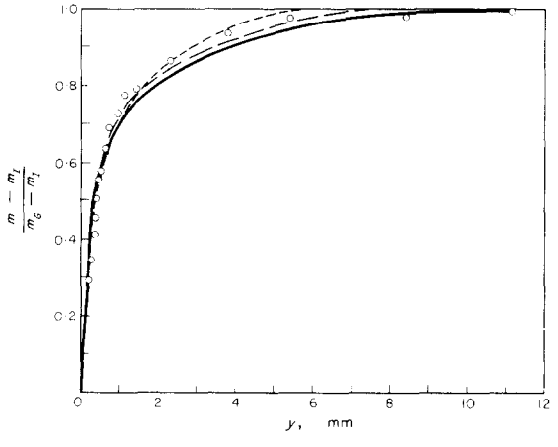

FIG. 4. Species concentration profile. Run No. 120, $M = 0{\cdot}0017$. —— Cebeci model; ——— Kays model; -- Launder *et al.* model; ○ Experiment.

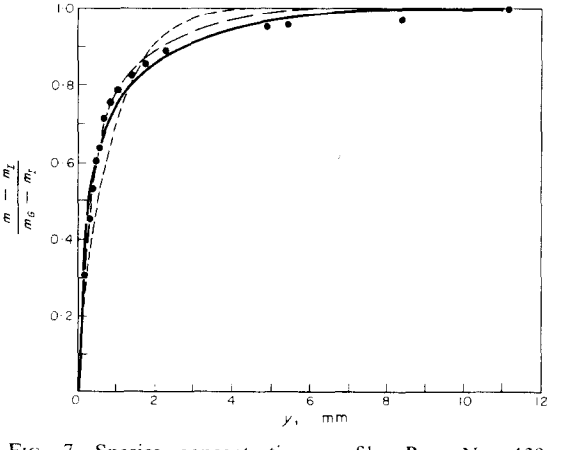

FIG. 7. Species concentration profile. Run No. 139, $M = 0{\cdot}0032$. —— Cebeci model; ——— Kays model; -- Launder *et al.* model; ● Experiment.

Table 2. Stanton numbers for heat and mass transfer

Run number	Experiment [4]			Prediction—Cebeci model		Prediction—$k-\varepsilon$ model	
	M	St_m	St_h	St_m	St_h	St_m	St_h
109	0·00071	0·0029	0·0035	0·0030	0·0034	0·0028	0·0032
111	0·00066	0·0027	0·0034	0·0027	0·0031	0·0026	0·0030
113	0·0013	0·0033	0·0040	0·0033	0·0036	0·0031	0·0033
115	0·0012	0·0030	0·0037	0·0031	0·0034	0·0029	0·0031
118	0·0017	0·0041	0·0039	0·0041	0·0038	0·0036	0·0033
120	0·0017	0·0039	0·0036	0·0039	0·0036	0·0036	0·0032
122	0·0023	0·0041	0·0039	0·0039	0·0036	0·0036	0·0032
125	0·0021	0·0036	0·0035	0·0035	0·0037	0·0031	0·0032
131	0·0023	0·0036	0·0038	0·0036	0·0037	0·0031	0·0032
135	0·0027	0·0039	0·0041	0·0039	0·0040	0·0033	0·0033
139	0·0032	0·0049	0·0046	0·0048	0·0045	0·0041	0·0035
144	0·0035	0·0051	0·0048	0·0052	0·0046	0·0042	0·0036

In the case of the model of Launder and Priddin the agreement is also not so satisfactory for, although the lower condensation rate flow predictions are in reasonable accord with the measurements, some large discrepancies between the predicted and measured profiles are evident for the higher rate. The disagreement is also reflected in the predictions of the Stanton numbers for heat and mass transfer where the model leads to values which are too low by about 35 per cent for the higher condensation rate. Launder and Priddin's model purports to include the effects of mass transfer and pressure gradients in terms of τ_+—in view of its simplicity an attractive concept—and has led to good results for a wide range of constant fluid property flows. However, the results obtained here show that some modification of the model is necessary if it is to account properly for the variable fluid properties and very large mass-transfer rates presently encountered.

Figures 8–13 display the predictions obtained with the model of Cebeci, the $k-\varepsilon$ model predictions and the measured profiles of velocity, temperature and concentration. Figures 8–10 correspond to the lower condensation rate flow and figures 11–13 to the higher. The predicted profiles obtained with the $k-\varepsilon$ model are in reasonable accord with the measured values and any disagreement can be explained in terms of experimental error and by the uncertainty in the specification* of the initial profiles of u, k and ε needed to start the computation. The level of agreement obtained with the $k-\varepsilon$ model is roughly comparable with that of Cebeci's model.

*This uncertainty in specification, while having some small effects on the detailed shape of the predicted profiles has little effect on the predicted values of mean heat- and mass-transfer rates.

In Table 2 values of the Stanton numbers for heat and mass transfer predicted with Cebeci's model and the $k-\varepsilon$ model are compared with the measured values for a range of condensation rates. It may be seen the results obtained with Cebeci's model are in excellent accord with the measurements; the maximum discrepancy between the measured and predicted values of Stanton numbers for heat transfer and mass transfer being about 10 and 5 per cent respectively. In the case of the $k-\varepsilon$ model the accuracy of the predictions is not quite so good and there is some evidence that the model underpredicts both the condensation rate and heat-transfer rate for the higher condensation rates. Here however the discrepancy is only just outside the estimated experimental error.

Some computations were also made to investigate the influence of the film on the predictions by setting the film thickness to zero. However, for the present problem it turns out that the film exerts only a small influence on the averaged condensation and heat-transfer rates. Typically, neglect of the film resulted in a predicted increase in the condensation rate of about 5 per cent and a reduction of about the same magnitude in the heat-transfer rate. Changes of similar nature were also observed when the bouyancy forces were omitted from the vapour–air mixture boundary-layer equations.

CONCLUDING REMARKS

The foregoing section has presented predictions of the condensing flow of a CCl_4 vapour–air mixture over a vertical plate. Of the mixing length models employed that of Cebeci [5] leads to results which are in almost all cases in good agreement with the measurements. However, the models of Kays [6] and Launder and Priddin [7] were less successful and some modification

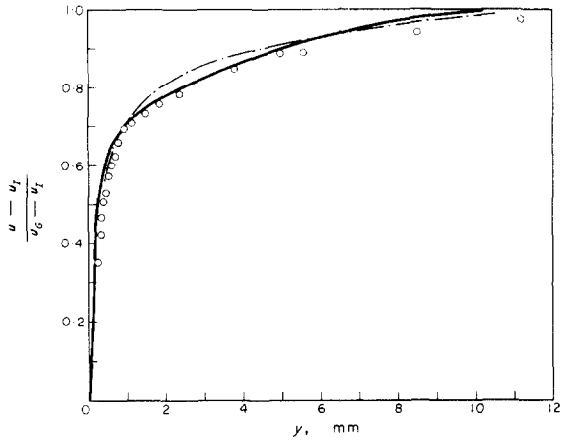

FIG. 8. Velocity profile. Run No. 120, $M = 0{\cdot}0017$. —— Cebeci model; —·— k,ε model; ○ Experiment.

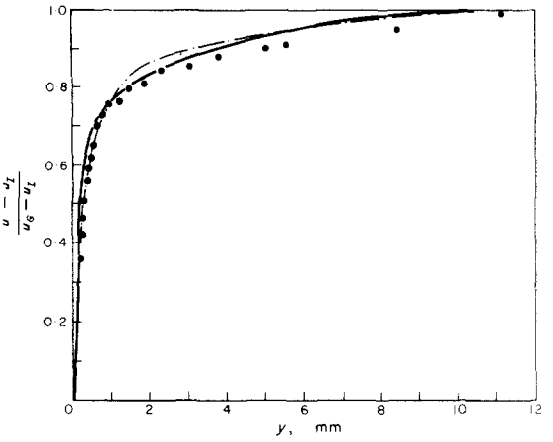

FIG. 11. Velocity profile. Run No. 139, $M = 0{\cdot}0032$. —— Cebeci model; —·— k,ε model; ● Experiment.

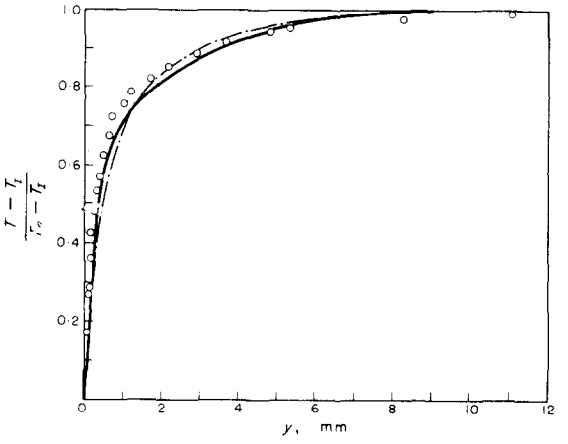

FIG. 9. Temperature profile. Run No. 120, $M = 0{\cdot}0017$. —— Cebeci model; —·— k,ε model; ○ Experiment.

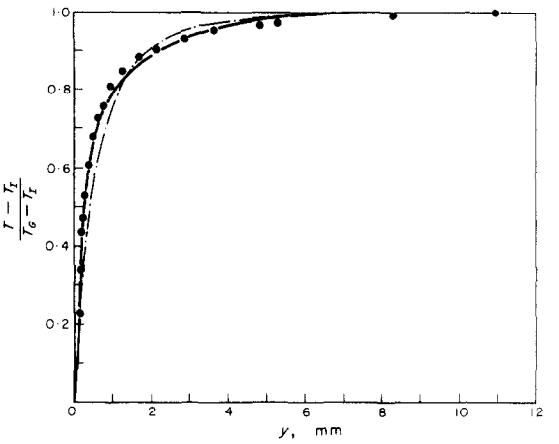

FIG. 12. Temperature profile. Run No. 139, $M = 0{\cdot}0032$. —— Cebeci model; —·— k,ε model; ● Experiment.

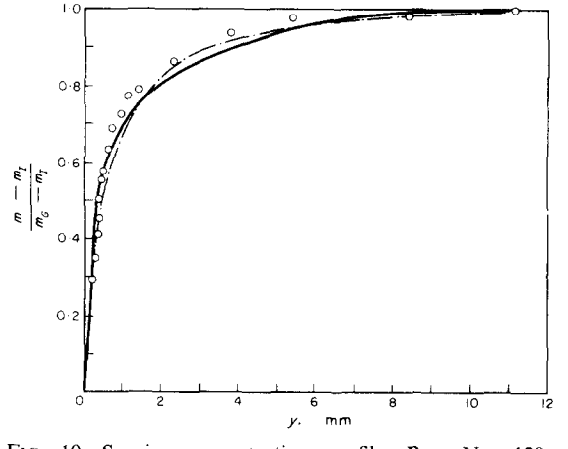

FIG. 10. Species concentration profile. Run No. 120, $M = 0{\cdot}0017$. —— Cebeci model; —·— k,ε model; ○ Experiment.

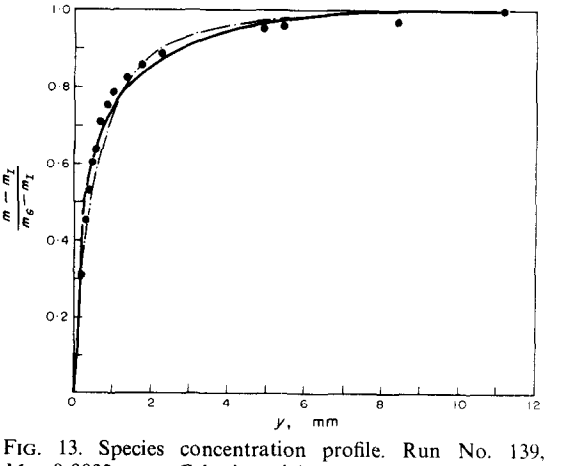

FIG. 13. Species concentration profile. Run No. 139, $M = 0{\cdot}0032$. —— Cebeci model; —·— k,ε model; ● Experiment.

of these models is clearly necessary if they are to account correctly for the behaviour of variable property flows with large condensation rate.

The $k-\varepsilon$ model has also performed tolerably well especially since the disposable empirical constants appearing in it were chosen to secure agreement with standard high Reynolds-number constant fluid property flows in the absence of either pressure gradient or mass transfer. The model has previously been applied to the successful prediction of range of flows with appreciable pressure gradients and surface mass-transfer rates [14] and [15] and may therefore be applied with some confidence to condensation problems in which a streamwise pressure gradient is present. Finally, it is appropriate to mention some possible extensions of the present work. In many condensation problems of practical significance the liquid film will be turbulent and it would seem profitable to extend the theory to include this. Of course, the Nusselt approximation would probably not then be appropriate and the full boundary-layer equations would have to be solved for the liquid film.

It may be expected that waves on the surface of the film would also exert some influence but this could be accounted for by allowing finite values of k and at the liquid–vapour interface. The $k-\varepsilon$ model also allows some account to be taken for the effects of high free stream turbulence intensities which commonly arise in condensation problems. For example, Priddin [21] has used the model to correctly predict the observed increase in heat-transfer rates to a turbine blade with increasing free stream intensity. It thus seems reasonable to hope that the model will reliably describe the influence of high free stream turbulence intensities in condensation problems.

Acknowledgements—One of the authors (W. P. Jones) wishes to acknowledge financial support from the Alexander von Humboldt-Stiftung during the period in which the present work was carried out. All the numerical computations have been performed by means of digital computers under the control of the computing centre of the Technische Hochschule Aachen.

REFERENCES

1. W. Nusselt, Die Oberflächenkondensation des Wasserdampfes, *Z. Ver. Dt. Ing.* **60**, 541–546, 569–575 (1916).
2. E. M. Sparrow and S. H. Lin, Condensation heat transfer in the presence of noncondensable gas, *J. Heat Transfer* **86**, 430–436 (1964).
3. V. E. Denny, A. F. Mills and V. J. Jusionis, Laminar film condensation from a steam–air mixture undergoing forced flow down a vertical surface, *J. Heat Transfer* **93**(3), 297–304 (1971).
4. H. Dallmeyer, Stoff- und Wärmeübertragung bei der Kondensation eines Dampfes aus einem Gemisch mit einem nichtkondensierenden Gas in laminarer und turbulenter Strömungsgrenzschicht, *ForschHft. Ver. Dt. Ing.* **539**, 4–24 (1970).
5. T. Cebeci, Behavior of turbulent flow near a porous wall with pressure gradient, *AIAA Jl* **8**(12), 2152–2156 (1970).
6. W. M. Kays, Heat transfer to the transpired turbulent boundary layer, *Int. J. Heat Mass Transfer* **15**, 1023–1044 (1972).
7. B. E. Launder and C. H. Priddin, The near wall mixing length profile—a comparison of some variants of Van Driest's proposal, Imperial College, Dept. Mech. Engng, London, TM/TN/A/15 (1971).
8. W. P. Jones, Laminarisation in strongly accelerated boundary layers, Ph.D.-Thesis, University of London (1971).
9. E. R. Van Driest, One turbulent flow near a wall, *J. Aeronaut. Sci.* **23**(11), 1007/1011 (1956).
10. U. Renz, Die Verdunstung an feuchten Oberflächen nach einer Darstellung im Mollier-Enthalpie, Zusammensetzungs-Diagramm und nach neuen Berechnungen, *Kältetechnik-Klimatisierung* **24**, 29–44 (1972).
11. U. Renz, Messungen und Berechnungen von adiabaten Oberflächentemperaturen bei der Verdunstung einer katalytisch zerfallenden Flüssigkeit in einen heißen Gasstrom, *Wärme- und Stoffübertragung* **6**, 215–220 (1973).
12. W. P. Jones and B. E. Launder, On the prediction of laminarescent turbulent boundary layers, ASME paper 69-HT-13 (1969).
13. B. E. Launder and W. P. Jones, Sink flow turbulent boundary layers, *J. Fluid Mech.* **38**, 817–831 (1969).
14. W. P. Jones and B. E. Launder, The prediction of laminarisation with a two-equation model of turbulence, *Int. J. Heat Mass Transfer* **15**, 301–314 (1972).
15. W. P. Jones and B. E. Launder, The calculation of low-Reynolds-number phenomena with a two-equation model of turbulence, *Int. J. Heat Mass Transfer* **16**, 1119–1130 (1973).
16. *VDI-Wärmeatlas*. VDI, Düsseldorf (1969).
17. R. C. Reid and T. K. Sherwood, *The Properties of Gases and Liquids*. McGraw-Hill, New York (1966).
18. H. B. Smits, Der Wärme- und Stoffaustausch beim Verdunsten am waagerechten Rohr bei natürlicher Konvektion, Dissertation TH München (1966).
19. Y. S. Touloukian, *Thermal Conductivity—Nonmetallic Liquids and Gases*, Vol. 3. Heyden and Son, London (1970).
20. S. V. Patankar and D. B. Spalding, *Heat and Mass Transfer in Boundary Layers*. Morgan–Grampian, London (1967).

CONDENSATION SUR UNE SURFACE VERTICALE A PARTIR D'UN ECOULEMENT TURBULENT

Résumé—On présente quelques estimations numériques concernant l'écoulement turbulent d'un mélange de vapeur de CCl_4 et d'air le long d'une paroi verticale sur laquelle la vapeur se condense. On résout par une procédure aux différences finies le système d'équations aux dérivées partielles qui gouvernent

la conservation de la quantité de mouvement, des espèces et de l'enthalpie. Les conditions aux limites à l'interface liquide air–vapeur sont obtenues à partir d'une modification de l'approximation de Nusselt pour le film liquide.

On obtient des résultats avec trois versions du modèle de la longueur de mélange de Prandtl et avec un modèle dans lequel la viscosité turbulente est déterminée à partir de la résolution des équations de transport pour l'énergie cinétique turbulente et pour le taux de dissipation de l'énergie turbulente – le modèle $k-\varepsilon$. Parmi les modèles à longueur de mélange, celui de Cebeci conduit au meilleur accord avec les mesures. Les prévisions du modèle $k-\varepsilon$ sont aussi en bon accord avec l'expérience.

KONDENSATION AUS EINER TURBULENTEN STRÖMUNG AN EINER SENKRECHTEN OBERFLÄCHE

Zusammenfassung—Der Aufsatz behandelt Berechnungsverfahren für den Wärme- und Stoffübergang bei der Kondensation von CCl_4 aus turbulenter Strömung eines CCl_4-Dampf-Luft-Gemisches an einer senkrechten Oberfläche. Das die Austauschvorgänge beschreibende Gleichungssystem wird durch ein Differenzverfahren gelöst und die Randbedingungen dabei durch eine modifizierte Nusselt'sche Wasserhauttheorie festgelegt.

Drei Vorschläge auf der Grundlage der Prandtl'schen Mischungswegtheorie und ein Ansatz, bei dem die turbulente Zähigkeit aus der Lösung zweier zusätzlicher Gleichungen für die kinetische Energie und die Dissipationsenergie der Turbulenz—k-ε-Modell—berechnet wird, werden geprüft.

Es zeigt sich, daß von den Mischungswegansätzen der von Cebeci am besten mit den Meßergebnissen übereinstimmt und daß das k-ε-Modell ebenfalls brauchbar ist.

КОНДЕНСАЦИЯ ПАРА НА ВЕРТИКАЛЬНОЙ ПЛАСТИНЕ В ТУРБУЛЕНТОМ ПОТОКЕ

Аннотация — Приводятся некоторые численные расчеты турбулентного потока CCl_4 — паровоздушной смеси с конденсацией пара на вертикальной пластине. Для паровоздушной смеси с помощью метода конечных разностей решена система дифференциальных уравнений в частных производных сохранения количества движения, массы и энтальпии. С помощью модифицированного приближения Нуссельта для жидкой пленки определены граничные условия на поверхности раздела: жидкость/воздух-пар.

Получены результаты для трех вариантов модели пути смешения Прандтля и для модели, в которой турбулентная вязкость определяется решением уравнений переноса для турбулентной кинетической энергии и скорости диссипации турбулентной энергии ($\kappa-\varepsilon$ модель). Среди моделей длины смешения наилучшее соответствие между экспериментом и теорией наблюдается в модели Чебечи. Расчеты по $\kappa-\varepsilon$ модели также хорошо согласуются с экспериментом.